Computers and Fluids 122 (2015) 66–82

Contents lists available at ScienceDirect

Computers and Fluids

journal homepage: www.elsevier.com/locate/compfluid

Free-surface film flow over topography: Full three-dimensional finite element solutions

S. Veremieiev [a,*], H.M. Thompson [b], P.H. Gaskell [a]

[a] School of Engineering and Computing Sciences, Durham University, Durham DH1 3LE, UK
[b] School of Mechanical Engineering, University of Leeds, Leeds LS2 9JT, UK

ARTICLE INFO

Article history:
Received 19 November 2014
Revised 12 August 2015
Accepted 14 August 2015
Available online 1 September 2015

Keywords:
Liquid film flow
Finite elements
Topography
Long-wave approximation
Navier–Stokes

ABSTRACT

An efficient Bubnov–Galerkin finite element formulation is employed to solve the Navier–Stokes and continuity equations in three-dimensions for the case of surface-tension dominated film flow over substrate topography, with the free-surface location obtained using the method of spines. The computational challenges encountered are overcome by employing a direct parallel multi-frontal method in conjunction with memory-efficient out-of-core storage of matrix co-factors. Comparison is drawn with complementary computational and experimental results for low Reynolds number flow where they exist, and a range of new benchmark solutions provided. These, in turn, are compared with corresponding solutions, for non-zero Reynolds number, from a simplified model based on the long-wave approximation; the latter is shown to produce comparatively acceptable results for the free-surface disturbance experienced, when the underpinning formal restrictions on geometry and capillary number are not exceeded.

1. Introduction

Processes involving the motion of liquid films on various substrates are encountered across engineering, the sciences and technology, as reported in the recent comprehensive review by Craster and Matar [1]. Examples from nature include the control of disease in plants [2], and the redistribution of the liquid linings of respiratory systems [3]. They form an important component across several industrial sectors, including the coating of papers and plastics in the inkjet and photographic industries [4], heat exchanger and combustion chamber design [5,6], and the application of anti-reflective coatings [7]. They are also crucial in the cooling of electronic devices [8], and in the manufacture of micro-scale electronic components, for example in direct-write printing of circuits [9], where the precise deposition of liquid films flowing over a distribution of functional topographic features (such as polymer light-emitting species on a screen) is vital to ensuring acceptable product quality and performance.

The ever-increasing requirements for predictable product and process properties has generated considerable interest in improving the understanding of complex free-surface film flows over topography. In many practically-important situations these requirements translate into the need for reliable film thickness control. This is often very difficult to achieve since free-surface disturbances induced by small-scale topography can result in film thickness non-uniformities that persist over length scales several orders of magnitude greater than the size of the topography itself [10]; other related experimental investigations of note supporting this include those of [8,11–14]. While well suited to studying the flow over isolated or periodically repeating topographical features, the routine use of experiments in the context of product and/or process design can prove prohibitive both cost and time wise; hence the recourse, over the last decade or so, to modelling approaches coupled with the efficient numerical solution of the associated governing equations.

From a consideration of the three-dimensional nature of the flows of interest and the disparity in length-scales encountered, the majority of models to emerge are based on application of the long-wave approximation which utilise the feature that the undisturbed asymptotic film thickness is small compared to the characteristic in-plane length scale. The additional neglect of inertia enables such flows to be represented either by a fourth order non-linear degenerate partial differential equation for the film thickness, or by a coupled set of second order equations for the film thickness and pressure [15], albeit with formal restriction to surface tension-dominated flows having small capillary number and for which the topography depth/height is small compared to the film thickness. These, so-called, lubrication equations have been used successfully to model thin film flows for a range of problems including flows with evaporation [16], with surfactants [17], in the presence of an electric field [18], and for the case of rivulet formation [19]. The influence of inertia can also be important in terms of the magnitude of the free-surface disturbances that

* Corresponding author. Tel.: +447943501632.
E-mail address: s.veremieiev@gmail.com (S. Veremieiev).

http://dx.doi.org/10.1016/j.compfluid.2015.08.016
0045-7930/

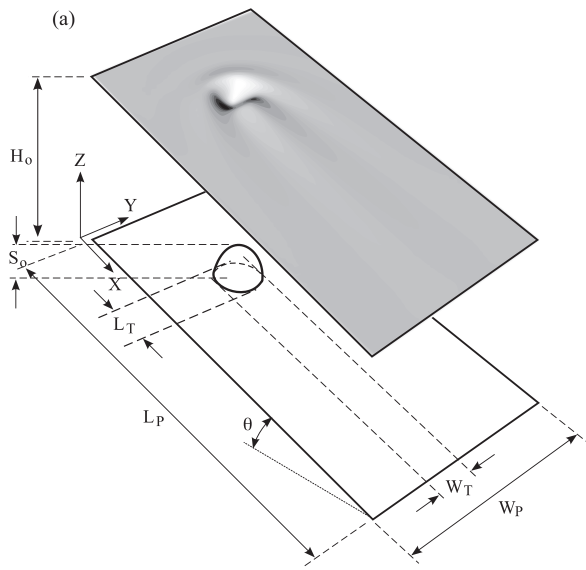

Fig. 1. Schematic diagram of gravity-driven film flow over a planar substrate containing a well-defined (a) hemispheroid and (b) trench topography; showing the coordinate system adopted and surface geometry.

form [20], and beyond a critical Reynolds number from the point of view of flow stability [21,22].

Despite their proven usefulness, the above models lack the generality associated with solving the governing Navier–Stokes and continuity equations themselves, which are not restricted in terms of choice of film thickness, size of capillary number or topography depth/height; another constraint lifted is that topographical features with perfectly steep sides can be accommodated without the need for smoothing. As might be construed, there are very few such film flow solutions in the literature; the exceptions being boundary element solutions obtained for Stokes flow, as reported by Pozrikidis, and Thoroddsen [23] and Blyth, and Pozrikidis [24] for flow over a small particle and a three-dimensional obstacle, respectively, and by Baxter et al. [25,26] for flow past hemispheric obstacles with large free-surface disturbances. Latterly [14], obtained solutions with inertia present for film flow over a bi-periodically repeating substrate using a Volume of Fluid algorithm to investigate pattern formation and mixing; see also the work of [27] which addresses the capillary flow problem of dynamic wetting as an interface forming process.

The remainder of the paper is organised as follows. The three-dimensional flow problems considered are described in Section 2, which includes the governing equation set, with the corresponding finite element formulation and method of solution described in Section 3. A series of results demonstrating the power and accuracy of the solution strategy adopted and the flow phenomena that are induced are provided in Section 4. Finally, conclusions are drawn in Section 5.

2. Problem specification

The problems considered are for the case of steady-state, gravity-driven, free-surface film flow down a planar substrate, inclined at an angle $\theta(\neq 0)$ to the horizontal, and containing hemispheroid or trench like topographical features, see Fig. 1, of height/depth S_0, streamwise diameter/length L_T and spanwise diameter/width W_T. The liquid is assumed to be incompressible and to have constant density, ρ, dynamic viscosity, μ, and surface tension, σ. The chosen Cartesian streamwise, X, spanwise, Y, and normal, Z, components of the coordinate vector, $\boldsymbol{X} = X\boldsymbol{i} + Y\boldsymbol{j} + Z\boldsymbol{k}$, are as indicated; $\boldsymbol{i}, \boldsymbol{j}, \boldsymbol{k}$ are the corresponding basis vectors of the coordinate system. The solution domain is bounded from below by the substrate, $Z = S(X, Y)$, from above by the free surface, $Z = F(X, Y)$, upstream and downstream by the inflow, $X = 0$, and outflow, $X = L_P$, planes, respectively, and to the left and right by the side planes at $Y = 0$ and $Y = W_P$. The film thickness, $H(X, Y)$, at any point in the (X, Y) plane is given by $H = F - S$. The resulting laminar flow is described by the Navier–Stokes and continuity equations, namely:

$$\rho \boldsymbol{U} \cdot \nabla \boldsymbol{U} = -\nabla P + \nabla \cdot \boldsymbol{T} + \rho \boldsymbol{G}, \tag{1}$$

$$\nabla \cdot \boldsymbol{U} = 0, \tag{2}$$

where $\boldsymbol{U} = U\boldsymbol{i} + V\boldsymbol{j} + W\boldsymbol{k}$ and P are the fluid velocity and gauge pressure, respectively; $\boldsymbol{T} = \mu(\nabla \boldsymbol{U} + (\nabla \boldsymbol{U})^T)$ is the viscous stress tensor, $\boldsymbol{G} = G_0(\sin\theta \boldsymbol{i} - \cos\theta \boldsymbol{k})$ is the acceleration due to gravity where G_0 is the standard gravity constant.

Taking the reference length scale in all directions to be the asymptotic, or fully developed, film thickness, H_0, and scaling the velocities by the free-surface (maximum) velocity apropos the classic Nusselt solution [28], $U_0 = \rho G_0 H_0^2 \sin\theta / 2\mu$, and the pressure (stress tensor) by $P_0 = \mu U_0 / H_0$, Eqs. (1) and (2) can be rewritten in non-dimensional form as:

$$\mathrm{Re}\, \boldsymbol{u} \cdot \nabla \boldsymbol{u} = -\nabla p + \nabla \cdot \boldsymbol{\tau} + \mathrm{St}\boldsymbol{g}, \tag{3}$$

$$\nabla \cdot \boldsymbol{u} = \boldsymbol{0}, \tag{4}$$

where $\boldsymbol{x} = x\boldsymbol{i} + y\boldsymbol{j} + z\boldsymbol{k}$, $\boldsymbol{u} = u\boldsymbol{i} + v\boldsymbol{j} + w\boldsymbol{k}$, p, $\boldsymbol{\tau}$ and $\boldsymbol{g} = \boldsymbol{G}/G_0$ are the non-dimensional coordinate, velocity, pressure, viscous stress tensor and gravity component, respectively; $\mathrm{Re} = \rho U_0 H_0 / \mu$ is the Reynolds number and $\mathrm{St} = \rho G_0 H_0^2 / \mu U_0 = 2/\sin\theta$ is the Stokes number.

The general problem definition is complete following the specification of appropriate no-slip, inflow/outflow, kinematic and free-surface normal and tangential stress boundary conditions, see [29]:

$$\boldsymbol{u}|_{z=s} = 0, \tag{5}$$

$$h|_{x=0} = 1, \quad \boldsymbol{u}|_{x=0,l_p;y=0,w_p} = z(2-z)\boldsymbol{i}, \tag{6}$$

$$(\boldsymbol{n} \cdot \boldsymbol{u})|_{z=f} = 0, \tag{7}$$

$$-p|_{z=f} + (\boldsymbol{\tau}|_{z=f} \cdot \boldsymbol{n}) \cdot \boldsymbol{n} = \frac{\kappa}{\mathrm{Ca}}, \tag{8}$$

$$(\boldsymbol{\tau}|_{z=f} \cdot \boldsymbol{n}) \cdot \boldsymbol{t} = 0, \tag{9}$$

where h, s, f together with l_p and w_p correspond to their dimensional counterparts, $\boldsymbol{n} = (-\frac{\partial f}{\partial x}\boldsymbol{i} - \frac{\partial f}{\partial y}\boldsymbol{j} + \boldsymbol{k}) \cdot [(\frac{\partial f}{\partial x})^2 + (\frac{\partial f}{\partial y})^2 + 1]^{-1/2}$